

Fig. S1. *Vibrio cholerae* wild-type excision. N16961 (serogroup O1 biotype El Tor), O395 (O1 classical) and MO2 (O139). *Vibrio cholerae* SG-7 (O56) does not contain VPI-1 or VPI-2 and served as a negative control.

Fig.S2. A. Conserved domains of IntV1 and IntV2. Amino acid alignment of IntV1 (gi: 9655299) and IntV2 (gi: 15641762) using the MUSCLE algorithm in Jalview. Both integrases share three conserved domains (represented by blocks in sequential order): DUF4102 (pfam13356) domain (IntV1: 5-94, IntV2: 8-97), SAM-like domain (pfam14659) (IntV1: 103-151, IntV2: 106-157) and the C-terminal domain contained a P4 catalytic domain (pfam00589) (IntV1: 213-390, IntV2: 215-393). The highly conserved active site residues are marked by triangles. **B.** Predicted secondary structure of N-terminus VpiT and TorI. In search for an unannotated RDF, the HHPred server identified a 52 amino acid region near the N-terminus of VpiT as having a distant relationship to TorI, a previously characterized excisionase. Although the shared identity in this region was 12% and the e-value of 0.0061, the predicted secondary structures of these regions were near identical.

Fig. S3 Mobile integrative genetic element (MIGE) recombination modules. A comparison of the genetic organization of the two *V. cholerae* VPIs examined in this study with the bacteriophage λ and the *E.coli* prophage KpIE1. Contrary to bacteriophage λ the integrases of the VPIs and KpIE1 possess promoter regions that overlap with attachment sites, making them accessible for regulation by intasome binding proteins. Additionally, the genetic organization reveals that the RDF(s) and integrase of VPI-2 and KpIE1 are not co-regulated as they are in bacteriophage λ . The

position of *vefB* also exposes the gene for possible regulation by intasome binding proteins.

Fig. S4 VefA and VefB bind the 1st half *attL2* site at a higher affinity. A.

Representation of the 1st and 2nd half fragments of the *attL2* DNA sequence, amplified with primer pairs attL2Fwd/attL2BRev and attL2CFwd/attL2Rev, respectively (Table S1), used for electrophoretic mobility shift assays (EMSAs). **B.** Varying concentrations of VefA (0 – 46 μ M) with *attL2* 1st half (30 ng) and 2nd half (30 ng). Binding is observed at 23 μ M for the first half. **C.** Varying concentrations of VefB (0 - 23.1 μ M) with *attL2* 1st half (30 ng) and 2nd half (30 ng). Binding is observed at 2.8 μ M and 2.4 μ M for the 1st and 2nd half, respectively. **D.** EMSA using control *V. vulnificus* DNA (30 ng) with varying concentrations of VefA (0 – 12 μ M) and VefB (0 - 4.19 μ M). No binding was observed.

Fig. S5. Distribution of Vefs in Bacteria. A BLAST analysis revealed over 3,000 representatives (among 105 genera and 283 species) with equal to or greater than 70% query cover and 40% identity to the *V. cholerae* RDFs. A visual representation of these results was created using the Krona visualization tool (59). Link to interactive view: <file:///C:/Users/Megan%20Carpenter/Desktop/Crosstalk%20Paper/Krona/FamilyGenusNopecies.html?dataset=0&node=0&collapse=true&color=false&depth=2&font=11&key=true>

Fig. S6. *Vibrio* island regions inserted at tmRNA genes containing RDFs. A) Island regions of *V. cholerae* and other Vibrionaceae which contain IntV1 homologs inserted at tmRNA genes as well as Vef homologs. Note the genetic variation of the gene content of each island. *Vibrio vulnificus* island (VVI) - 5. **B)** Strain name with % homology to *V. cholerae* N16961 IntV1 and RDFs VefA, VefB or VefC. These

observations suggest an evolutionary relationship between IntV1 and the Vefs, supporting the VPI-1 cross-talk hypothesis.

Table S1. Primers used in this study

Primer Name	Sequence (5' → 3')	Product size (bp)
Mutant Construction		
VC0817A	tctagaAAGCTGCGATAGGGAGCT	520
VC0817B	ACCACAGCGTCGACATACGAG	
VC0817C	<u>CTCGTATGTCGACGCTGTGGT</u> ATCAAGAAAGAGCGGTTTCAAG	561
VC0817D	gagctcGGCTAACGTCCCTATAGTC	
VC0817FF	AGCTCTTCCATCGACAACACCTCT	2,200
VC0817FR	TCGCCAGTGGAAGCAGAGCA	
VC0847A	tctagaTAGCCATTTCGTTAGCGTGTC	556
VC0847B	ATCGTCTTGTGGATCGATGC	
VC0847C	<u>GCATCGATCCACAAGACGAT</u> AGAGGTAGCCTATCTGTGAC	548
VC0847D	gagctcTGAGGATCCATGATATCCGC	
VC0847FF	CTAGCTTCCGCTTGTAAAGAC	2,287
VC0847FR	TACTAACGGGTATCGAACTC	
cnVC1758A	tctagaGATTTCGGTGAGTTGTCCGAG	531
cnVC1758B	TTGCCATGAGCGAGAATTGC	
cnVC1758C	<u>GCAATTCTCGTCTATGGCAA</u> GGAAGTTACAGTGTGGCTGG	578
cnVC1758D	gagctcTCAGTAAACAGAAAGGCTGCC	
cnVC1758FF	AAGCAAACGCACTCAATGCG	2,285
cnVC1758FR	CTGGTCGACAAGATTGTCTG	
VC0497A	GtctctagaGTACTCTTGCGATGCGTTTGG	541
VC0497B	TCGTAGAAATTCATGGGAATTGTC	
VC0497C	<u>GACAATTCCTCATGAGATTTCTACGA</u> GAATCCTTTTCAGTAACACAAACATC	554
VC0497D	CgagctcCGCTTCAACCGCTAACAGGT	
VC0497FF	CGAACACAACCCACCTTCCAACC	1,345
VC0497FR	GAGTCTGAACAACCTGATTGG	
Excision Assays (<i>attP</i>)		
InvVC0847B	ATCGTCTTGTGGATCGATGC	744
Inv/NestVC0817R2	GCATCACCACATTCTCATAAC	
NestVC0847F3	TTTCTCTCTAGGTTTGGAGG	483
NestVC0817R3	CTCTGTCCATAGACACCCAG	
VPI-2 InvVC1808F	AGCTAGACAGATTAGCTAACC	1,352
CnVC1758B	TTGCCATGAGCGAGAATTGC	
NestVC1758comR	AGAATTGCTTGGACGTACGC	461
NestVC1809comF	GCGTAACTGAGAAAAGTGTG	
Excision Assays (<i>attB</i>)		
VPI-1 attBF1	ATAGGGAGCTGGGCGTTAAT	428
VPI-1 attBR1	TGTAAGACGGGGAAATCAGG	
VPI-1 attBF2	TTGATGAGACGCTCTGAACC	217
VPI-1 attBR2	ATTCGTTAGCGTGTCCG	
VPI-2 fk1	CTGGCTATGAGCTGATTTG	1,449
VPI-2 fk2	AGGGATTGGCTTTGAGG	
VPI-2attF	AGAGTAAAAGTCGCCAAAGC	524
VPI-2attR	GGGTGCAATTTTCGCATGTTGC	
Complementation		
VC0847F	gagctcAGGTACTACTACAAGGTACAC	1,385
VC0847R	tctagaAGCGTATTCCACTGACAACC	

VC1758F	ggtaccGAGCTCGCTTTGAATATAGG	1,303
VC1758R	gagctcGAGTCCTCATGCTCTAGCCAG	
VC1785F	tctagaGGCATGCTGGTGTGTTACTAC	414
VC1785R	tctagaGACGCATGTATAATCACGC	
VC1809F	gagctcGTGGTTGATAGGCAATTGCAC	414
VC1809R	ctgcagGATCACACAAGTAAACCAGC	
VC0497F	gagctcCAGTGGCGGCTTATCCATGG	293
VC0497R	ctgcagCAGCGCCCTGTTGATGATGT	
Protein Expression		
BamHIVC1785R	CTCGGATCCTCATCGCTGTTTAAGAC	225
NcoIVC1785F	TGCCCATGGATGGGACAACAAGACATAG	
VefAmutRev	CATGGACTGAAAATACAGG	
VefAmutFwd	GGACAACAAGACATAGGAG	
NcoIVefBFwd	TGCCCATGGGATTGCAACTAACCAACCTGAG	251
BamHIVefBRev	CTCGGATCCCTAATCCATTGACGATTGG	
Binding Assays		
attL2Fwd	TCTCACTCACCGCCACATTCAA	327
attL2Rev	GCCATTTCAATCCCTCAAGT	
attR1Fwd	GATGGGTACACCAGATTAACACG	190
attR1Rev	CCCCAGCTCCACCAAATCATAG	
attL2BRev	GTGGGTAGCTGGGTATTACTT	
attL2CFwd	AAGTAATACCCAGCTACCCAC	
VV1_0809A	tctagaAGCCAGGGTTTAACTACCGC	440
VV1_0809B	GGCTGAGTAAGCACGTTGA	

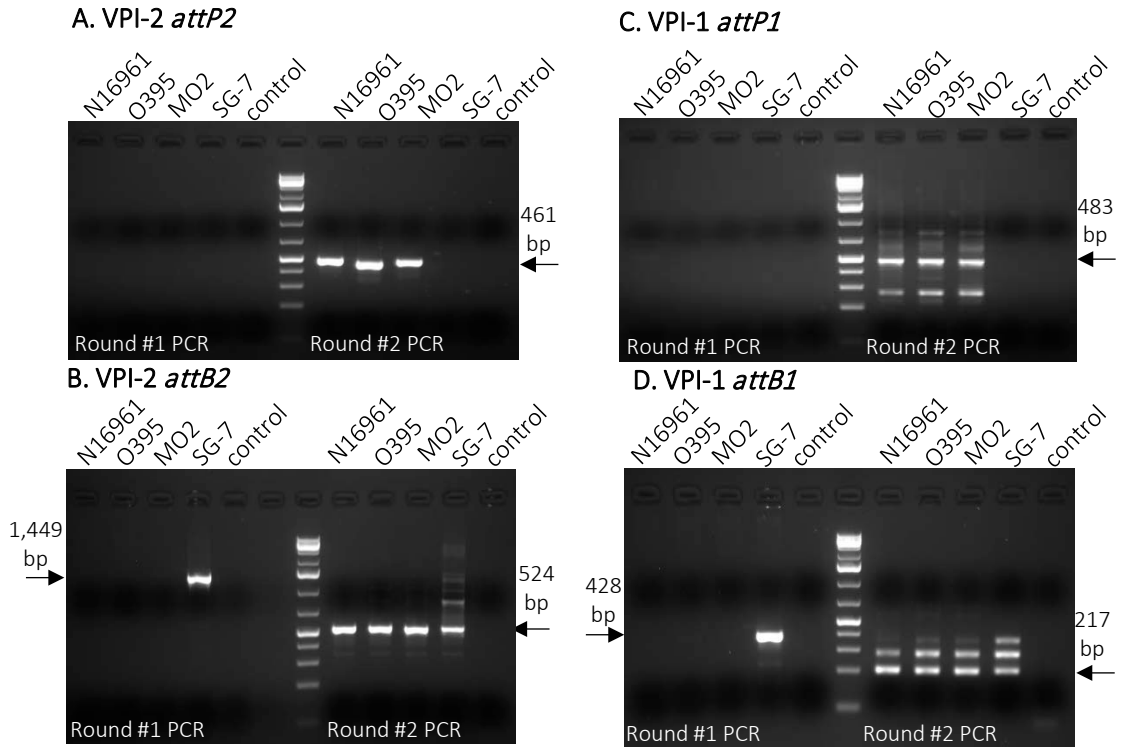
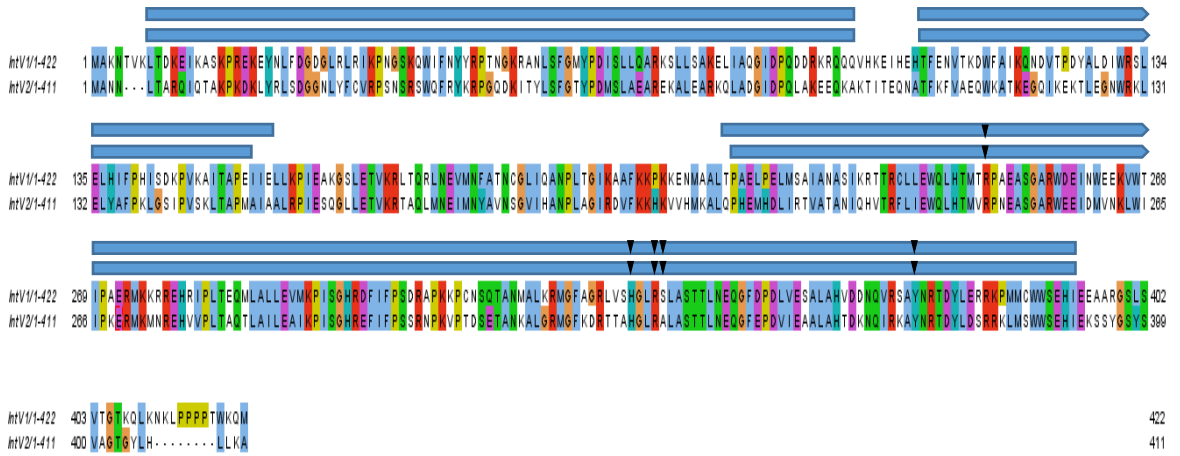


Figure S1

A. IntV1 and IntV2 sequence alignment



B. IntV1 and IntV2 sequence alignment

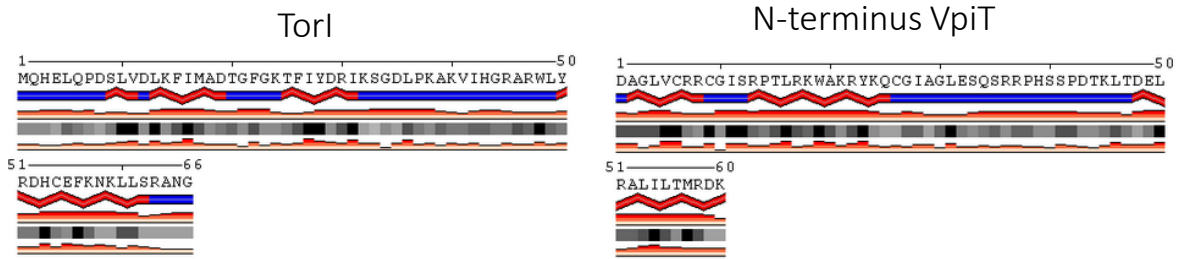


Figure S2

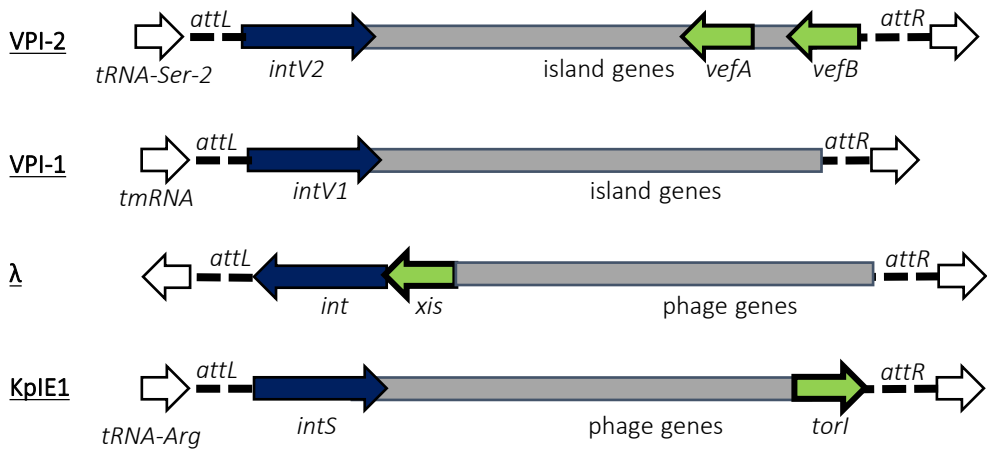
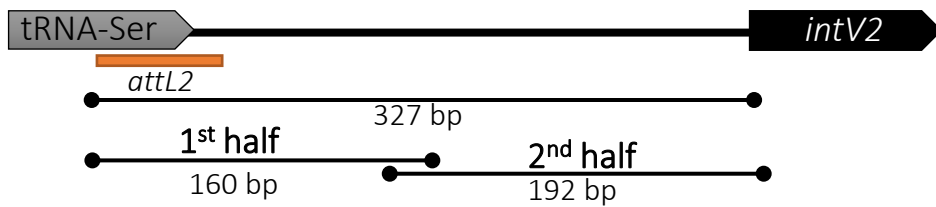
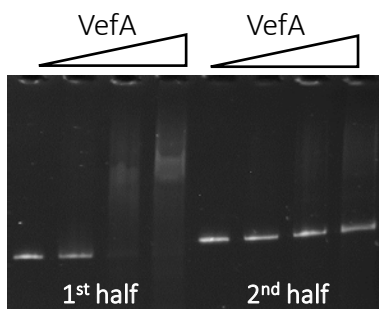


Figure S3

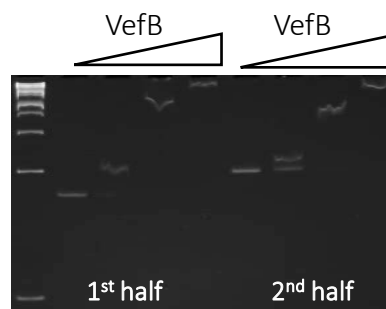
A



B



C



D

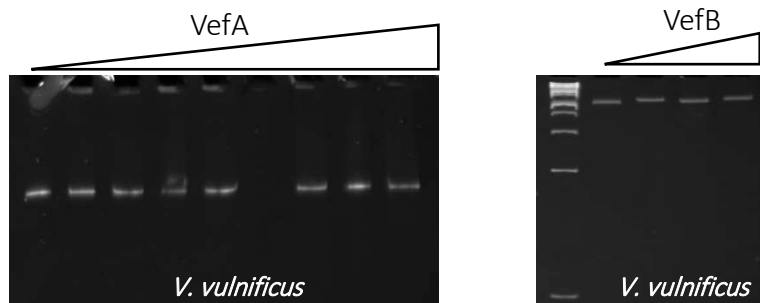
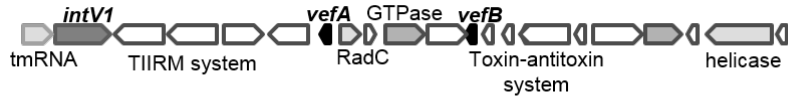


Figure S4

A

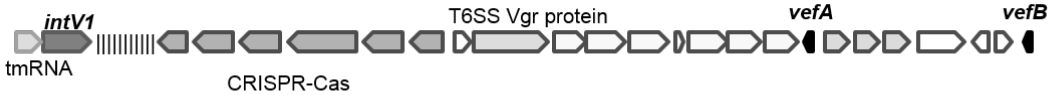
Vibrio cholerae sv Inaba 12129(1)



Vibrio cholerae CT 5369-93



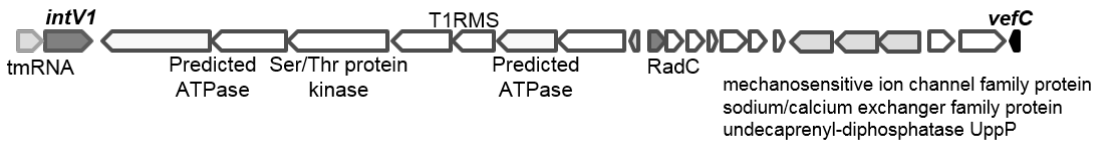
Vibrio cholerae sv. O135 RC385



Listonella anguillarum sv. O1 96F



Vibrio cholerae HE-09



Vibrio diazotrophicus NBRC 103148



Vibrio vulnificus YJ016 VVI-V



B

Strain	IntV1	VefA	VefB	VefC
<i>V. cholerae</i> sv Inaba 12129(1)	93%	99%	83%	
<i>V. cholerae</i> CT 5369-93	81%			98%
<i>V. cholerae</i> sv. O135 RC385	100%	91%	97%	
<i>Listonella anguillarum</i> sv. O1 96F	82%			94%
<i>V. cholerae</i> HE-09	81%			100%
<i>V. diazotrophicus</i> NBRC 103148	81%			94%
<i>V. vulnificus</i> YJ016	81%	88%		

Figure S6